THE JOURNAL OF PHYSICAL CHEMISTRY C

Article

pubs.acs.org/JPCC

Gold Nanowires: A Time-Dependent Density Functional Assessment of Plasmonic Behavior

GiovanniMaria Piccini,[†] Remco W. A. Havenith,[‡] Ria Broer,[‡] and Mauro Stener*[,§,∥,⊥]

[†]Institut für Chemie, Humboldt-Universität zu Berlin, Unter den Linden 6, 10099 Berlin, Germany

[‡]Zernike Institute for Advanced Materials, University of Groningen, Nijenborgh 4, 9747 AG Groningen, The Netherlands

[§]Dipartimento di Scienze Chimiche e Farmaceutiche, Università di Trieste, Via L. Giorgieri 1, I-34127 Trieste, Italy

[∥]Consorzio Interuniversitario Nazionale per la Scienza e Tecnologia dei Materiali, INSTM, Unita' di Trieste, I-34127 Trieste, Italy

[⊥]INFM DEMOCRITOS National Simulation Center, Trieste, Italy

ABSTRACT: The surface plasmon resonance has been theoretically investigated in gold nanowires by means of time-dependent density functional theory. Linear chains of Au atoms and nanowires with the structure of the fcc bulk gold grown along the ⟨110⟩ and ⟨111⟩ directions have been considered. The effects of changing the length and the section on the plasmon have been studied. Strong photoabsorption is found when the length is above 2 nm: in that case the absorption profile is characterized by a sharp peak, and its analysis reveals that many configurations contribute to the transition, confirming its collective nature as an s ← s intraband transition. As expected, the effect of increasing the length is reflected in a red shift of the plasmon.

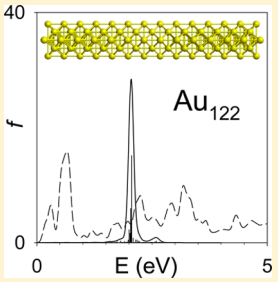

1. INTRODUCTION

In recent years the scientific interest toward gold nanosystems has grown dramatically,[1] one of the many reasons for the explosion of the research in this field can be identified as the specific optical properties of such systems. Moreover, it is worth mentioning the high ability of gold to form well-defined nanosized structures, whose shapes can be tuned and controlled, to some extent, already at the level of a conventional chemical synthesis.[2−7] This allows the synthesis of gold nanoclusters with defined shape and size distributions, which can be characterized with electron microscopy or X-ray diffraction techniques. The samples are usually in solution, and gold nanoparticles must therefore be stabilized with proper ligands: typically thiolates play a central role, due to their specific high tendency to form strong Au−S chemical bonds. Other protective agents, such as surfactants, can also be employed to stabilize nanoparticles with weaker chemical bonds.

The optical absorption of gold nanoparticles is characterized by a strong absorption band which, for sufficiently large sized nanoparticles, namely beyond 2 nm, falls in the visible region.[1] This feature is rather sensitive to specific characteristics of the sample, namely the particle size, its shape, the nature of the stabilizing ligand, and the nature of the solvent or the medium. Such a strong absorption corresponds to the surface plasmon resonance[8] (SPR) and is interpreted as a collective excitation of the conduction electrons of the metal particle. Because of the role of the SPR as an optical property of nanoparticles, the necessity has emerged to theoretically investigate such phenomenon, with the aim to understand its nature, to simulate and rationalize the experimental spectra, and, as a final ambitious goal, to perform a computational design of novel nanostructured materials with specific optical properties.

In this context, the first proposed and widely used method to simulate SPR is the Mie theory, which treats the light scattering by a conducting sphere in a purely classical manner. Although this approach is quite simple, computationally cheap, and qualitatively correct, it suffers from two obvious shortcomings: first the model does not consider at all the discrete atomic structure of the real nanoparticle which is treated as a homogeneous conducting medium, and second the model is based on classical electrodynamics and therefore quantum size effects are completely neglected. Moreover, Mie theory can be applied analytically only to spherical, ellipsoidal, and core−shell structures; if different shapes are considered, numerical techniques as electromagnetic finite differences time domain (FTTD)[9] or discrete dipole approximation (DDA)[10] must be employed.

In all cases, the applicability of classical electrodynamics methods (Mie theory, FTTD, and DDA) is limited to systems whose size is large enough to exclude quantum size effects, in practice for systems larger than 20 nm. However, sometimes the applicability of the DDA approach can be pushed to much smaller sizes, for example to study the optical properties of bimetallic clusters with various segregation types.[11]

The first step beyond classical theories is represented by the time-dependent local density approximation (TDLDA) implemented employing the jellium model:[12] the metal nanoparticle is described as a background consisting of a spherical

Received: June 11, 2013
Revised: July 24, 2013
Published: July 24, 2013

   dx.doi.org/10.1021/jp405769e | J. Phys. Chem. C 2013, 117, 17196−17204

positive charge density which models the average nuclear positions; such background supports the electrons which are treated with quantum mechanics. Of course, jellium misses the discrete atomic structure of the cluster, but the TDLDA formalism gives a quantum mechanical description of the electron excitations of the model system: the SPR is described as free electron oscillations. Moreover, the TDLDA jellium model offers a practical and economical, still rather crude, tool to consider more specific effects which can be included in the theoretical model, namely the effect of an embedding medium to simulate, for example, the solvent effects.[13]

TDDFT implementations along the conventional quantum chemical linear combination of atomic orbital (LCAO) formalism represent a valid methodology to study plasmon resonance. The only problem is their computational cost which, at the moment, prevents to study clusters containing more than 100−200 gold atoms.[14−17] In any case, where practicable, the TDDFT LCAO methods are the best compromise between accuracy and computational economy with respect to other ab initio formalisms. Recently, also the linear response (LR) TDDFT implementation in the framework of the projector augmented wave (PAW) method[18] has allowed to calculate the photoabsorption spectrum of a Au_{144} cluster protected by thiolate ligands.[19] Plasmonic excitations of Au, Ag, and Cu clusters have been studied by LR methods as well.[20] It is worth mentioning that, despite LR, TDDFT can be implemented also accordingly to the time-evolution formalism, like in the OCTOPUS code,[21,22] such a scheme has been employed to study pure[23] and bimetallic[24] large clusters (up to 147 atoms). It is interesting to note that the time-evolution formalism does not suffer from the problem to extract a high number of eigenvalues of the spectrum, typical of the implementations based on the Casida[25] scheme. On the other hand, the time-evolution method does not allow any assignment of the spectral features to specific electron transitions; such an assignment is instead accessible when the Casida scheme is employed.

The first TDDFT study of noble metal nanowires is the work of Aikens[26] on silver nanorods, which gave a clear rationalization of the nature of the plasmon resonance: an intense transition whose collective nature is revealed by its mixed composition of many configurations and its high oscillator strength due by the "constructive" interference of the dipole transition moments of each configuration. For gold nanowires similar results have been obtained by Liao et al.[27] although the authors did not analyze the mechanism which led to the plasmon appearance in detail. Quite interestingly, a study on thin nanowires consisting of chains of silver and gold atoms[28] revealed that the most intense "longitudinal" absorption peaks correspond to the HOMO−LUMO transition, missing the typical collective nature of the plasmon. Such behavior was already pointed out by Salek in a previous work.[29] An important contribution for the assessment of plasmon in molecules and clusters has been given very recently by Bernadotte et al.:[30] they proposed to study the evolution of the TDDFT photoabsorption spectra by changing a scalar factor $0 \leq \lambda \leq 1$ used to "turn on" the coupling matrix **K**. With this approach the authors have been successful to discriminate between single-particle and plasmon excitations in various systems like metal chains and clusters, alkene chains, and fullerenes. We will employ some ideas from this scaling approach analysis for the discussion of the present results.

In the present work a series of gold nanowires of different sizes and thickness have been considered in order to study the emergence of the plasmon absorption peak as a function of the nanowire size and shape and its rationalization in terms of electronic structure in a systematic way. Moreover, we have considered two different growing typologies of the nanowires, namely the ⟨110⟩ and the ⟨111⟩ directions. In fact, transmission electron microscope (TEM) data analysis has shown that gold nanowires can grow along both ⟨110⟩[31] and ⟨111⟩[32] directions.

Although most of the experiments are actually relative to gold nanoparticles protected by ligands, we have restricted our study to bare gold cluster. In fact, the phenomenology, at least as the SPR is concerned, is essentially an effect of the gold core. Of course, ligands can induce relevant changes on the electronic structure of the metallic core and, as a consequence, on the optical spectra. However, in this study, we preferred to put our attention to the simplest systems which carry the essence of the phenomenon and consider only length, section, and growing directions variations along the series.

2. THEORETICAL METHOD

The first step consists of a conventional scalar relativistic (SR) self-consistent field (SCF) Kohn−Sham (KS) calculation, employing a finite basis set of Slater type orbitals (STO), with the ADF code.[33,34] It is well-known that the inclusion of relativistic effects is mandatory to describe properly the electronic structure of gold compounds,[35] so we have employed the SR zero-order regular approximation (ZORA) formalism.[36]

The results of the SR-KS calculation (KS eigenvalues and orbitals) are then used as input for the TDDFT section. The TDDFT approach for electronic excitations and its implementation in the ADF code have been described in detail in the literature,[37] so here we just recall the salient steps.

The general problem is cast in the following eigenvalue equation:[25]

$$\mathbf{\Omega F}_I = {\omega_I}^2 \mathbf{F}_I \tag{1}$$

where $\mathbf{\Omega}$ is a four indices matrix with elements $\mathbf{\Omega}_{ia\sigma,jbr}$; the indices consist of products of occupied-virtual (ia and jb) KS orbitals, while σ and τ refer to the spin variable. The eigenvalues ${\omega_I}^2$ correspond to squared excitation energies while the oscillator strengths are extracted from the eigenvectors $\mathbf{F}_I$.[25] The $\mathbf{\Omega}$-matrix elements can be expressed in terms of KS eigenvalues (ε) and the coupling matrix **K**:

$$\Omega_{ia\sigma,jb\tau} = \delta_{\sigma\tau}\delta_{ij}\delta_{ab}(\varepsilon_a - \varepsilon_i)^2 + 2\sqrt{(\varepsilon_a - \varepsilon_i)}\, K_{ia\sigma,jb\tau} \sqrt{(\varepsilon_b - \varepsilon_j)} \tag{2}$$

The elements of the coupling matrix **K** are given by

$$K_{ij\sigma,kl\tau} = \int \mathrm{d}\mathbf{r} \int \mathrm{d}\mathbf{r}'\, \varphi_{i\sigma}(\mathbf{r})\varphi_{j\sigma}(\mathbf{r})\left[\frac{1}{|\mathbf{r}-\mathbf{r}'|} + f_{xc}^{\sigma\tau}(\mathbf{r}, \mathbf{r}', \omega)\right]\varphi_{k\tau}(\mathbf{r}')\varphi_{l\tau}(\mathbf{r}') \tag{3}$$

where the φ are the KS orbitals and $f_{xc}^{\sigma\tau}(\mathbf{r},\mathbf{r}',\omega)$ is the exchange-correlation kernel. In this work the kernel is approximated according to the adiabatic local density approximation (ALDA).[38]

3. COMPUTATIONAL DETAILS

In the present work we have taken the Au−Au experimental interatomic bulk distance of 2.88 Å to build all the structures under study; it is worth mentioning that test TDDFT

dx.doi.org/10.1021/jp405769e | J. Phys. Chem. C 2013, 117, 17196−17204

calculations have been performed also on small clusters previously optimized using LDA XC-functional showing no significant differences with respect to the nonoptimized ones reported in this work. The TDDFT calculations have been performed at the bulk geometries, implying also that all calculated spectra correspond to vertical excitations. In fact, it has been shown in previous work that structural relaxation has a very limited impact on the calculated photoabsorption spectra.[15] For all the calculations we have employed a basis set of STO functions of DZ type with frozen core up to the 4d subshell for Au. This choice has been justified in a previous work[14] where the effect of the basis set on the photoabsorption of gold clusters has been studied at the TDDFT level with both DZ and TZP basis. It was found that the spectra calculated with DZ and TZP basis were in practice identical, therefore validating the choice of DZ basis set. It is worth noting that the choice of DZ basis set in TDDFT calculations of Au and Ag clusters is widely customary.[15,16,26,28]

All the calculations have been performed employing the LB94[39] exchange-correlation potential, since it is well-known that to obtain accurate TDDFT valence electron spectra, it is necessary to employ an exchange correlation potential with the correct Coulomb asymptotic behavior;[40] such a feature is properly supported by LB94. Moreover, LB94 has proven to give accurate photoabsorption spectra with respect to the experiment for gold clusters[15] as well as gold−silver nanoalloys.[16]

All calculations have been performed with the version 2010.02 of the ADF code. A critical point of the present TDDFT approach is the number of the lowest eigenvalues (roots) to be extracted from eq 1. In fact, such a number has a decisive impact on the computational effort required for the calculation and must be adequate in order to have a proper description of the calculated spectrum, since it controls the upper limit of the excitation energy range. Moreover, when many eigenvalues are extracted, numerical stability problems may arise and a stricter criterion for the SCF convergence has been found to help in this respect. Therefore, we have employed a threshold of 10^{-8} for the maximum element of the commutator between the Fock and the density matrix in the representation of the basis functions. The clusters considered in this work are all neutral and have a closed-shell ground state electronic configuration.

4. RESULTS AND DISCUSSION

4.1. Gold Linear Chains. The first systems considered are linear chains of gold atoms of increasing size: Au_{14}, Au_{20}, and Au_{30} whose lengths are 3.744, 5.472, and 8.352 nm, respectively. These systems are very appealing because their $D_{\infty h}$ symmetry makes the computations very cheap, and their lengths, exceeding by far 2 nm, should be long enough to generate strong plasmonic behavior. In Figure 1 we report the calculated spectra up to 6 eV as well as the figures of the nanowires. A fundamental and still debated question is whether the observed spectral feature can be ascribed to a plasmon resonance or to a conventional one-electron transition. We have referred in the Introduction to the scaling approach proposed by Bernadotte,[30] which consists of repeating the TDDFT calculations several times with different values of the scaling factor λ in the range $0 \leq \lambda \leq 1$. In this way it is possible to follow the plasmon, whose excitation energy is much more sensitive to λ than the single-particle excitations. The procedure is very effective; however, it becomes prohibitive for

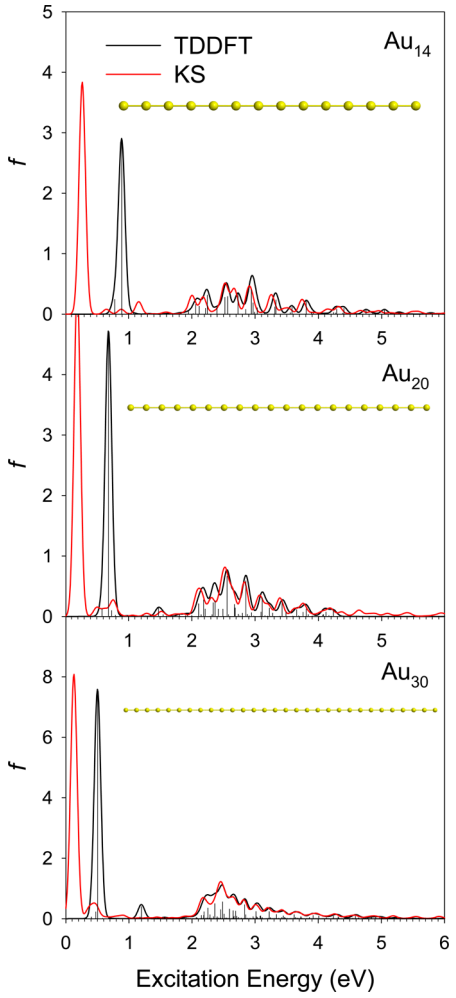

Figure 1. TDDFT (black curve) and KS (red curve) spectra of linear chains of gold atoms (Au_{14}, Au_{20}, and Au_{30}) convoluted with a Gaussian function of fwhm = 0.12 eV. The vertical bars correspond to the TDDFT discrete transitions. The structures are shown as insets.

applications on very large systems where one single TDDFT calculation can already be very demanding. For this reason we adopted a simplified version of this analysis, which consists of comparing the TDDFT spectrum with a spectrum calculated at Kohn−Sham level, where the excitation energy corresponds to the KS eigenvalue difference and oscillator strength is calculated from dipole transition moments between KS orbitals. We refer to such spectrum as the KS spectrum. In comparison with the scaling approach of Bernadotte, TDDFT and KS spectra correspond to $\lambda = 1$ and $\lambda = 0$, respectively, so we consider only the two extremes of the λ interval. This simplified scheme is computationally very cheap since the KS spectrum calculation does not require the TDDFT machinery but can be obtained immediately after the SCF resolution of the KS equations. Therefore, the analysis can be applied to large systems with negligible computational cost in addition to a single TDDFT calculation.

In Figure 1 the TDDFT results are reported as vertical bars (representing discrete transitions) which have been also broadened with Gaussian functions of fwhm = 0.12 eV (black curve). The KS spectrum has been calculated as well, and in Figure 1 only the broadened (fwhm = 0.12 eV) KS spectrum are reported for analysis reasons (red curve). It is important to remember that two dipole active electronic transitions may take

dx.doi.org/10.1021/jp405769e | J. Phys. Chem. C 2013, 117, 17196−17204

place in a closed shell linear molecule, classified according to the "longitudinal" Σ_u and the "transversal" Π_u dipole components. Although both components have been calculated and inserted in the figure, only the "longitudinal" Σ_u ones contribute in practice to the spectrum, since the "transversal" Π_u excitations are extremely weak. The TDDFT spectra give a strong peak at low energy which is red-shifted with increasing length (0.89, 0.68, and 0.48 eV for Au_{14}, Au_{20}, and Au_{30}, respectively), a typical behavior of plasmon resonance. In Table 1 the low-energy transitions are reported in order to analyze

Table 1. Calculated TDDFT Low-Energy Electronic Transitions of Au_{14}, Au_{20}, and Au_{30}, Excitation Energy (E_{EXC}) in eV, Absolute Oscillator Strength (f), and Assignment in Terms of One-Electron Excited Configurations

transition	E_{EXC} (eV)	f	assignment
Au_{14}			
$1\Sigma_u$	0.78	0.24	74% HOMO−2 → LUMO
$2\Sigma_u$	0.89	2.88	90% HOMO → LUMO
Au_{20}			
$1\Sigma_u$	0.58	0.13	73% HOMO−2 → LUMO
$2\Sigma_u$	0.68	4.65	94% HOMO → LUMO
Au_{30}			
$1\Sigma_u$	0.40	0.06	71% HOMO−2 → LUMO
$2\Sigma_u$	0.48	0.24	49% HOMO → LUMO+1 46% HOMO-1 → LUMO+2
$3\Sigma_u$	0.50	7.44	96% HOMO → LUMO

their nature: the strong peak is always ascribed mainly to the HOMO → LUMO transition. Interestingly, as the nanowire length increases, the HOMO → LUMO nature of the excitation becomes more and more pronounced (90%, 94%, and 96% for Au_{14}, Au_{20}, and Au_{30}, respectively). Such observation should rule out the plasmonic nature of such a strong transition; in fact, being ascribed to a single HOMO → LUMO transition, it misses completely any collective character typical of plasmon resonances. It is worth noting, however, that at variance with what one would have been expected in terms of eigenvalue difference the HOMO → LUMO transition is not the lowest transition in the spectrum, but it is the second one in Au_{14} and Au_{20} and the third one in Au_{30}. This finding suggests that the coulomb kernel plays an important role in the excitation energy but, on the other hand, is not effective to couple with other transitions. The other low-energy transitions have an intensity which is 1 or 2 orders of magnitude lower than the HOMO → LUMO one. The molecular orbitals involved in such low-energy transitions all consist mainly of Au 6s atomic functions; therefore, the transitions can be designated as s ← s intraband transitions. Now let us consider the transitions at higher energy: in Au_{20} and Au_{30} we find a very weak isolated transition at 1.47 and 1.20 eV, respectively; they both belong still to the s ← s intraband group. Then, in the range from 2 to 5 eV for all the three nanowires here considered, a series of moderately weak but very dense transitions are found; their analysis reveals that they can all be assigned as s ← d interband transitions. Finally, we compare the TDDFT spectrum (black line) with the KS one (red line). We find very close resemblance for the s ← d interband transitions, revealing their one-electron nature, while for the s ← s intraband transitions we find an energy shift of the HOMO → LUMO transition to higher energy in the TDDFT with respect to the KS. We have already discussed about the energy shift of the HOMO → LUMO transitions; their intensity does not change appreciably between TDDFT and KS, in line with their one-electron nature.

In summary, we conclude this section saying that thin nanowires constituted by linear atom chains seemingly do not display any intense plasmonic resonance, even if their length exceeds 8 nm (Au_{30}), as demonstrated by the TDDFT analysis which does not reveal any collective behavior.

4.2. Gold Nanowires with ⟨110⟩ Growth Direction. The next class of systems considered are gold nanowires of finite size, with fcc bulk structure and grown along the ⟨110⟩ direction, whose shapes are shown as insets in Figure 2 for Au_{32} and Au_{50} and in Figure 3 for Au_{68}, Au_{86}, and Au_{122}.

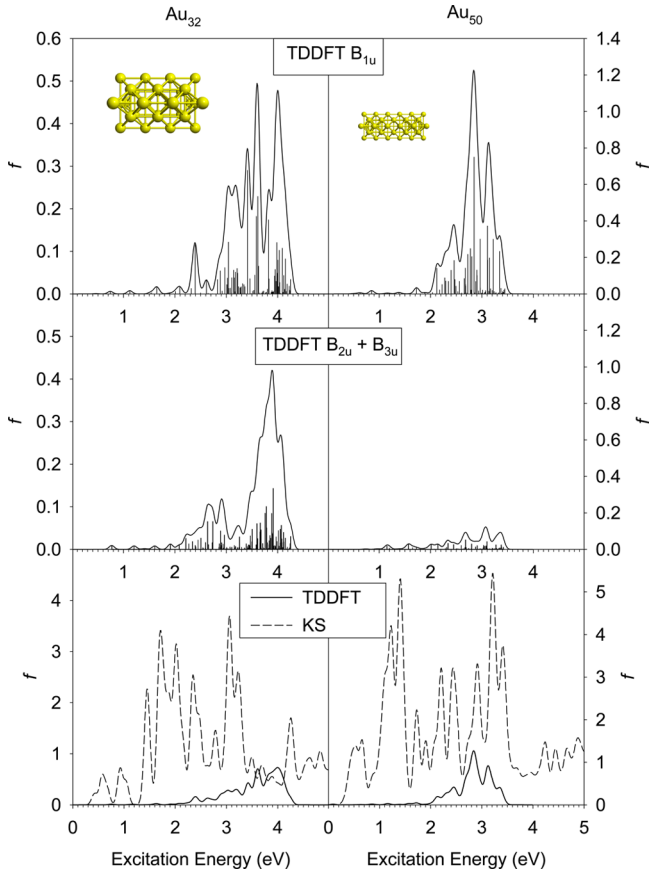

Figure 2. Photoabsorption spectra of gold nanowires grown along the ⟨110⟩ direction (Au_{32} left column and Au_{50} right column) convoluted with a Gaussian function of fwhm = 0.12 eV. The vertical bars correspond to the TDDFT discrete transitions. The structures are shown as insets. Upper panels: longitudinal transitions; central panel: transversal transitions; lower panel: comparison between TDDFT (full line) and KS (dashed line).

In Figure 2 we report the calculated TDDFT spectra for Au_{32} (left column) and Au_{50} (right column). Let us start the discussion of the results with Au_{32}, considering first that the length of this nanowire is only 0.864 nm, so we cannot reasonably expect any plasmonic behavior. In the upper panel the TDDFT spectrum is reported (both discrete lines and the profile smoothed by a Gaussian function with fwhm = 0.12 eV) for the longitudinal transitions corresponding to the B_{1u} dipole component. The low-energy part of the spectrum is rather empty; in fact, the first peak with appreciable intensity falls at

dx.doi.org/10.1021/jp405769e | J. Phys. Chem. C 2013, 117, 17196−17204

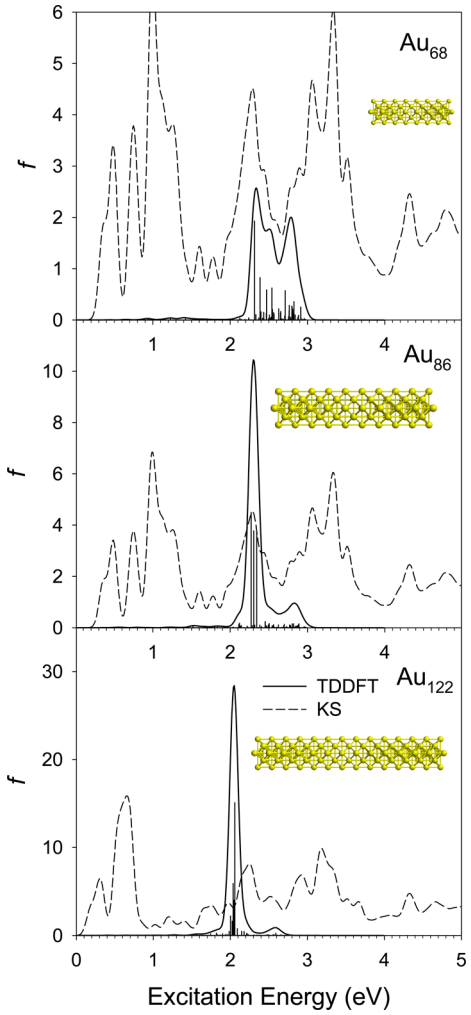

Figure 3. TDDFT (full line) and KS (dashed line) photoabsorption spectra of gold nanowires grown along the ⟨110⟩ direction (Au_{68}, Au_{86}, and Au_{122} from upper to lower panel) convoluted with a Gaussian function of fwhm = 0.12 eV. The vertical bars correspond to the TDDFT discrete transitions. The structures are shown as insets.

2.39 eV (with f = 0.116) and can be ascribed to a transition with a leading contribution of 59% from a single configuration whose character is due to an intraband sp ← sp transition. As the excitation energy increases above 2.8 eV, the discrete transitions gain intensity and become very crowded, giving rise to a broad band. The analysis of the most intense transitions indicates their strongly mixed nature. In some cases the leading configuration does not exceed 16%; the remaining contribution is spread over many configurations, each with very low contribution. In any case these transitions can be classified all as sp ← d interband: similar to the linear chains, as the energy increases the excitations originating from the d band start to play a more important role. The transversal dipole contributions to the spectrum (B_{2u} and B_{3u}) are considered together in the central panel. As can be observed the intensity is only slightly lower than in the longitudinal direction; the main difference is that the intensity increase takes place at 3.4 eV instead of 2.8 eV. The analysis of the most intense transitions encompassed by the first peak around 3.4 eV and by the maximum around 3.9 eV gives an sp ← d interband character for all the considered transitions. In the lower panel of Figure 2 the TDDFT spectrum (all dipole components, solid line) is compared with the KS spectrum (dashed line). It is quite surprising that the two spectra are completely different, with the KS profile showing high intensity between 1 and 3 eV, while the TDDFT in comparison is much weaker with a slowly increasing intensity from 3 to 4 eV. This behavior is completely different with respect to the linear chains of Au atoms (see section 4.1.), for which TDDFT and KS spectra were essentially the same, with the only exception of the HOMO → LUMO transition which was shifted by a few tenths of an electronvolt to higher energy in TDDFT with respect to KS. This finding suggests that for Au_{32} the static one-electron description completely fails to describe the spectrum, which therefore is strongly affected by response effects which are included in the TDDFT formalism and generate a quenching of the intensity with respect to the KS result ("screening").[41] Such response effects are reflected in the nature of the transitions, which cannot be described by a single excited configuration but rather as a mixing of several ones.

The next member of the series, Au_{50}, is considered in the right column of Figure 2. The length of this nanowire is 1.44 nm so it is still below the limit for the appearance of the plasmon resonance, which is around 2 nm. The longitudinal TDDFT results are reported in the upper panel. A maximum is found at 2.85 eV for a transition with f = 0.75; its nature is strongly mixed (each configuration contributes at most for 20%), and its character corresponds as usual to the sp ← d interband transition. With respect to Au_{32}, the intensity is larger by more than a factor of 2, and this is consistent with the larger size of the cluster. Going to the transversal contributions, the intensity becomes really negligible with respect to the longitudinal component, as a consequence of the aspect ratio. For this reason we will not consider anymore the transversal contribution in the next members of the series. Finally, in the lower box of Figure 2 the TDDFT and the KS spectra are compared; also in this case they look completely different from each other, with the TDDFT intensity still strongly quenched with respect to the KS one.

The next three members of the series (Au_{68}, Au_{86}, and Au_{122}) are considered all together in Figure 3, where the TDDFT spectrum is compared with the KS one. The results include all dipole components (longitudinal and transversal); however, the transversal intensity is much weaker than the longitudinal one so the total contribution coincides in practice with the longitudinal one.

The length of Au_{68} is 2.02 nm, so we are in the vicinity of the plasmonic regime; however, the relative TDDFT spectrum (upper panel of Figure 3) is still definitely less intense than the KS one although the quenching is now less strong than in the previous two members of the series Au_{32} and Au_{50}. The TDDFT spectrum of Au_{68} is dominated by the transition at 2.31 eV with f = 1.93, which is responsible for the first maximum. Such a transition is very mixed, contributed by many configurations with the leading one by only 18%; its character is mainly s ← s intraband with some p contamination. A second maximum is found around 2.8 eV consisting of many discrete excitations; the most intense falls at 2.71 eV with f = 0.57 and corresponds to a sp ← d interband transition. So for this system we have identified a very intense s ← s intraband transition, which is also very important in the low-energy region of the linear chains of Au atoms but is absent in the smaller nanowires Au_{32} and Au_{50}. So this observation suggests that this s ← s intraband transition could be an incipient plasmon resonance.

dx.doi.org/10.1021/jp405769e | J. Phys. Chem. C 2013, 117, 17196−17204

Now consider Au_{86} (central box of Figure 3): the cluster length is 2.59 nm so now we can expect to see a plasmon; in fact, the TDDFT spectrum shows a very focused peak around 2.3 eV with an intensity more than twice the corresponding KS intensity. It is worth noting that the peak consists essentially of only three transitions; at higher energy the transitions appear to be extremely weak with respect to the main peak. This findings are all consistent with a plasmonic nature of such resonance. More precisely, the three transitions are found at 2.27, 2.30, and 2.34 eV with intensity f = 4.49, 3.78, and 3.77, respectively. They are all strongly mixed, and again, from the analysis of the transitions, we can safely assign them to s ← s intraband transitions with some p contamination.

The next cluster is Au_{122} (lower panel of Figure 3); the length is now 3.744 nm, and we can expect an intense surface plasmon resonance. In fact, the TDDFT spectrum gives a very intense and focused peak, almost 1 order of magnitude more intense than the KS background. Such a peak is dominated by a single transitions, the other ones being all extremely weak. The dominating excitation is found at 2.06 eV with f = 15.10, and also in this case its character corresponds to an s ← s intraband transition with some p contamination. With respect to Au_{86}, the plasmon is red-shifted by 0.24 eV, from 2.30 to 2.06 eV; also this behavior is consistent with the behavior of SPR with respect to size for noble metal clusters.[42]

From the discussion of the results reported in Figure 3 we can trace the following observations regarding the rising of the plasmon resonance: (a) the plasmon resonance starts to appear when the cluster size is above 2 nm, (b) its appearance is revealed when its intensity starts to overcome that of the KS spectrum, (c) its nature is a mixing of many configurations and is attributed to a s ← s intraband transition with some p contamination, and (d) the plasmon is red-shifted as size increases.

With this analysis it is possible to identify the rising of the plasmonic behavior for clusters with finite section and with length above 2 nm as well as to exclude plasmonic behavior in the linear chains of gold atoms. So it is still interesting to study how the plasmon depends on changing the aspect ratio of the cluster, which corresponds to the ratio between cluster length and width; for this reason in Figure 4 we have considered another gold nanowire but with smaller radius, built by alternating a layer of 4 Au atoms with a layer of one single Au atom belonging to the {110} planes of fcc perpendicular to the ⟨110⟩ growth direction, keeping the D_{2h} point symmetry. Its length is 3.74 nm so it has the same length of the Au_{14} linear chain and of the previous Au_{122} nanowire but has a section which is intermediate between them. From the TDDFT spectrum we find immediately that the transversal dipole contributions are negligible and that a single longitudinal peak carries most of the intensity, in line with a plasmonic behavior. Also in this case the TDDFT intensity is about 1 order of magnitude larger than the KS one. The intense excitation is found at 1.73 eV with f = 14.17; its analysis reveals a strong mixing and is attributed to an s ← s intraband transition with some p contamination. It is therefore interesting to compare the spectra of the three nanowires with length 3.74 nm, namely Au_{14} (Figure 1, upper panel), Au_{66} (Figure 4, lower panel), and Au_{122} (Figure 3, lower panel). They have indeed several common features: (a) The KS spectrum is characterized by a strong a narrow peak at low energies (around 0.7 in Au_{66} and Au_{122}, around 0.3 eV in Au_{14}) followed by a flat, irregular, and less intense profile. (b) In the TDDFT the strong peak is shifted to higher energy: 0.9, 1.73, and 2.06 eV as the section increases while the intensity in the other energy region is reduced. (c) The intense TDDFT transition is always ascribed to an s ← s intraband transition with some p contamination. The observation (b) is less strict for Au_{14}; moreover, the mixed character of the intense transition is actually found only in Au_{66} and Au_{122}, while for Au_{14} it is ascribed to a pure HOMO → LUMO excited configuration. As a conclusion, we may say that, analogous to the linear gold chain, the transition for Au_{14} cannot be ascribed to a pure plasmon resonance since it misses completely any collective nature. However, it represents very well the extrapolation of the plasmon in a series of nanowires of decreasing section; so we may consider it as a "pseudoplasmon", a kind of a limit behavior for 1D objects of infinitesimal thickness.

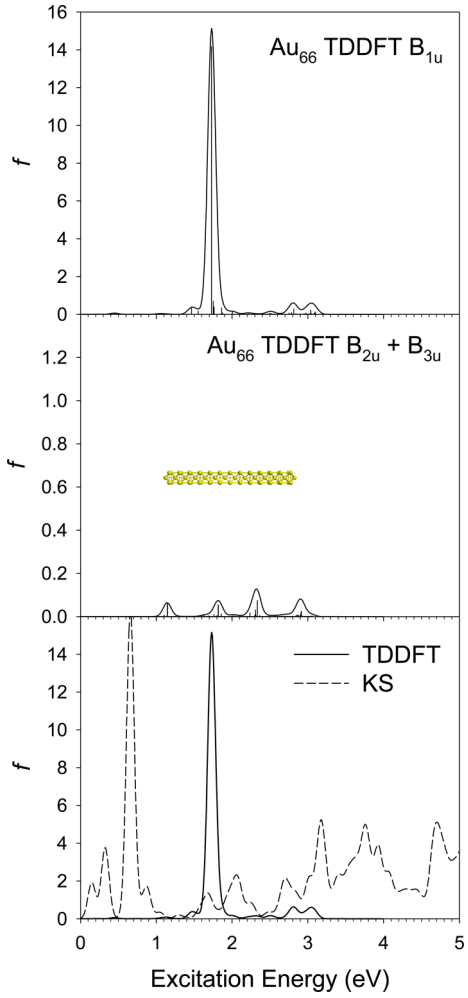

Figure 4. Photoabsorption spectra of gold nanowire Au_{66} grown along the ⟨110⟩ direction convoluted with a Gaussian function of fwhm = 0.12 eV. The vertical bars correspond to the TDDFT discrete transitions. The structure is shown as inset. Upper panel: longitudinal transitions, central panel: transversal transitions, lower panel: comparison between TDDFT (full line) and KS (dashed line).

4.3. Gold Nanowires with ⟨111⟩ Growth Direction. In Figure 5 we report the TDDFT results for the nanowires grown along the ⟨111⟩ direction: their structures have been built taking a layer of 7 atoms of the {111} plane (6 at the vertices of an hexagon plus the central one) inserted between two staggered layers consisting of 6 atoms arranged in a triangle (3 atoms at vertices and 3 atoms at edges). The structures are

dx.doi.org/10.1021/jp405769e | J. Phys. Chem. C 2013, 117, 17196−17204

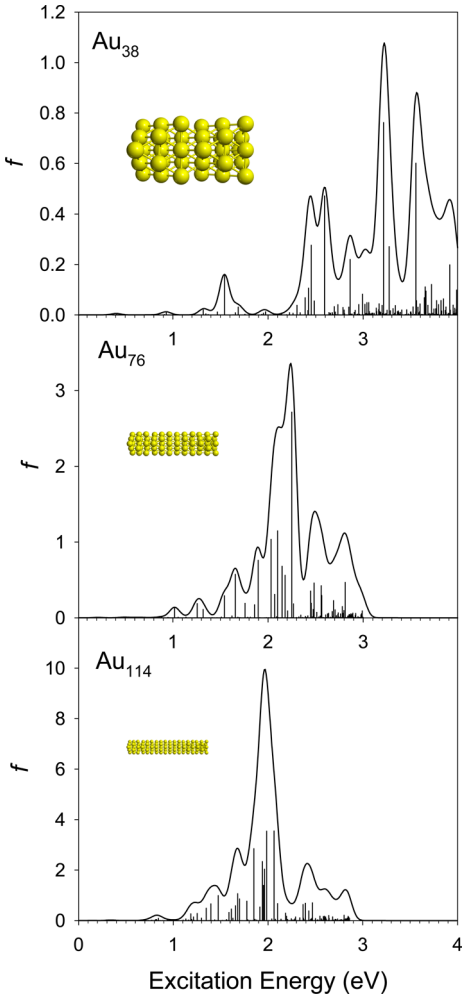

Figure 5. TDDFT photoabsorption spectra of gold nanowires grown along the ⟨111⟩ direction (Au_{38}, Au_{76}, and Au_{114} from upper to lower panel) convoluted with a Gaussian function of fwhm = 0.12 eV. The vertical bars correspond to the TDDFT discrete transitions. The structures are shown as insets.

reported as insets in the figure and belong to the D_{3d} point group symmetry. We do not consider the KS spectrum since the behavior of emerging plasmon has been already described in previous sections, and it holds for present case as well. The first member of the series is Au_{38} (upper panel of Figure 5); its length is 1.18 nm so we do not expect to find the plasmon resonance. The TDDFT spectrum gives various transitions. The most intense ones are all mixtures of many configurations: an isolated one at low energy (1.54 eV with $f = 0.16$) with sp ← sp intraband nature, while the next ones are quite close in energy. The transitions at 2.59 eV with $f = 0.47$ and at 3.21 eV with $f = 0.76$ are assigned to sp ← sp intraband transitions, while the one at 3.55 eV with $f = 0.60$ corresponds to a sp ← d interband excitation. This finding is consistent with the nature of the transitions already found in Au_{32} grown along the ⟨110⟩ direction with length 0.87 nm (upper panel of Figure 2) which are sp ← sp intraband below 2.8 eV and sp ← d interband above 3.4 eV.

The next system is Au_{76} (central panel of Figure 5) whose length is 2.59 nm, and therefore the plasmon is expected. In fact, a strong transition is found at 2.25 eV with $f = 2.72$. In this case it is dominated (43%) by a single configuration so it is not strongly mixed as usual; its nature is s ← s intraband. It is worth noting that two additional relatively strong excitations are present just above 2 eV; for this reason the peak is spread over 0.3 eV, at variance with Au_{86} grown along the ⟨110⟩ direction with comparable length (2.59 nm, central panel of Figure 2) whose plasmon peak width is only 0.1 eV. It seems that for ⟨111⟩ nanowires the plasmon is less focused than in ⟨110⟩ ones; this may be due to the lower symmetry (D_{3d} with respect D_{2h}) and to the less effective configuration mixing. In fact, the focusing of the intensity in a single transition can be efficiently obtained when a constructive interference among the excited configurations with high dipole transition moment generates a single transition which carries most of the oscillator strength.

The next member of this series is Au_{114} with a length of 4.00 nm, considered in the lower panel of Figure 5. The TDDFT spectrum displays a maximum just below 2 eV. In particular, there are two strong transitions with comparable intensity at 1.98 and 2.06 eV both with $f = 3.55$: the first one is strongly mixed (maximum contribution 15%), while the second one is less mixed (one configuration contributes for 44%); both are classified as s ← s intraband. It is important to note the presence of an intense transition downward to 1.85 eV, making the plasmon appear rather wide (more than 0.2 eV) in this case as well. We can conclude this section observing that for ⟨111⟩ nanowires the plasmon appears wider than for the ⟨110⟩ series as a consequence of the presence of a small number of transitions of comparable intensity. This reduced "focusing" may be ascribed to the lower symmetry of these nanowires leading to reduced configuration mixing in the composition of the transitions.

5. CONCLUSIONS

In this work the nature and the origin of the surface plasmon resonance (SPR) have been theoretically investigated in three series of gold nanowires by means of the TDDFT method. The three series are characterized by their structures: the first one consists of linear chains of gold atoms and the other two by nanowires with the structure of the fcc bulk gold grown along the ⟨110⟩ and ⟨111⟩ directions, respectively. For each series, the effect of increasing wire length on the emergence of the plasmonic behavior has been analyzed. For ⟨110⟩ nanowires the effect of the thickness has been considered as well. In order to investigate the plasmonic behavior, the TDDFT spectra have been compared with the KS ones, as limiting cases of the scaling method suggested by Bernadotte et al.[30] For the linear chains, we found that the TDDFT spectrum resembles closely the KS result, suggesting that response kernel plays only a minor role. The only difference is evident for the strong absorption at low energy (<1 eV) which is ascribed to a single excited configuration relative to the HOMO → LUMO which is shifted by few tenths of an electronvolt to higher energy in TDDFT with respect to KS. Therefore, we do not find any evidence of a collective behavior in linear chains, and we are led to exclude the presence of a plasmon in these systems.

For ⟨110⟩ nanowires we found strong absorption when their length is above 2 nm: in that case the TDDFT absorption is characterized by a sharp peak much more intense than the KS spectrum. This finding, together with the electron transition analysis, which reveals that the transition is contributed by many configurations, confirms its collective nature. The analysis of the involved orbitals ascribes the excitation to an s ← s intraband transition. As expected, the effect of increasing the length is reflected in a red shift of the plasmon. When the thickness effect is considered, it is found that the plasmon is

dx.doi.org/10.1021/jp405769e | J. Phys. Chem. C 2013, 117, 17196−17204

red-shifted when the thickness is reduced. Interestingly, it seems that the HOMO → LUMO transition in linear chains represents well an extrapolation of the plasmon to infinitesimal thickness. Similar trends are found for the nanowires grown along the ⟨111⟩ direction, although in this case the plasmon appears less focused, distributed on a wider energy range, and split over a small number of transitions of comparable intensity. This finding is concomitant with a less effective configuration mixing, probably due to the reduced symmetry with respect to the ⟨110⟩ ones.

In summary, the present study has traced a coherent picture of the SPR for bare gold nanowires, identifying the salient mechanisms behind the phenomenon. Future extensions of this work could be to study the behavior of plasmon resonances in more complex systems, like for example gold clusters protected by ligands like thiols or chemical substitutions of Au with Ag in various chemical ordering.

AUTHOR INFORMATION

Corresponding Author

*E-mail: stener@univ.trieste.it (M.S.).

Notes

The authors declare no competing financial interest.

ACKNOWLEDGMENTS

This work has been supported by grants from MIUR (Programmi di Ricerca di Interesse Nazionale PRIN 2010) of Italy, from Consorzio Interuniversitario Nazionale per la Scienza e Tecnologia dei Materiali (INSTM) (Progetto PRISMA 2004) and CNR of Rome (Italy), and from INFM DEMOCRITOS National Simulation Center, Trieste, Italy. R.W.A.H. acknowledges the Zernike Institute for Advanced Materials for financial support ("Dieptestrategie" program). The authors also acknowledge the HPC Europa2 programme (project 228398) providing most of the computing time at the SARA supercomputing center in Amsterdam.

REFERENCES

(1) Burda, C.; Chen, X.; Narayanan, R.; El-Sayed, M. A. Chemistry and Properties of Nanocrystals of Different Shapes. *Chem. Rev.* **2005**, *105*, 1025−1102.

(2) Sau, T. K.; Murphy, C. J. Seeded High Yield Synthesis of Short Au Nanorods in Aqueous Solution. *Langmuir* **2004**, *20*, 6414−6420.

(3) Nikoobakht, B.; El-Sayed, M. A. Preparation and Growth Mechanism of Gold Nanorods (NRs) Using Seed-Mediated Growth Method. *Chem. Mater.* **2003**, *15*, 1957−1962.

(4) Tsunoyama, H.; Nickut, P.; Negishi, Y.; Al-Shamery, K.; Matsumoto, Y.; Tsukuda, T. Formation of Alkanethiolate-Protected Gold Clusters with Unprecedented Core Sizes in the Thiolation of Polymer-Stabilized Gold Clusters. *J. Phys. Chem. C* **2007**, *111*, 4153−4158.

(5) Price, R. C.; Whetten, R. L. All-Aromatic, Nanometer-Scale, Gold-Cluster Thiolate Complexes. *J. Am. Chem. Soc.* **2005**, *127*, 13750−13751.

(6) Jin, R.; Qian, H.; Wu, Z.; Zhu, Y.; Zhu, M.; Mohanty, A.; Garg, N. Size Focusing: A Methodology for Synthesizing Atomically Precise Gold Nanoclusters. *J. Phys. Chem. Lett.* **2010**, *1*, 2903−2910.

(7) Qian, H.; Zhu, M.; Wu, Z.; Jin, R. Quantum Sized Gold Nanoclusters with Atomic Precision. *Acc. Chem. Res.* **2012**, *45*, 1470−1479.

(8) Noguez, C. Surface Plasmons on Metal Nanoparticles: The Influence of Shape and Physical Environment. *J. Phys. Chem. C* **2007**, *111*, 3806−3819.

(9) Kunz, K. S.; Luebbers, R. J. *The Finite Difference Time Domain Method for Electromagnetics*; CRC Press, LLC: Boca Raton, FL, 1993; pp 123−162.

(10) Draine, B. T.; Flatau, P. J. Discrete Dipole Approximation for Scattering Calculations. *J. Opt. Soc. Am. A* **1994**, *11*, 1491−1499.

(11) Logsdail, A. J.; Johnston, R. L. Predicting the Optical Properties of Core−Shell and Janus Segregated Au−M Nanoparticles (M = Ag, Pd). *J. Phys. Chem. C* **2012**, *116*, 23616−23628.

(12) Palpant, B.; Prével, B.; Lermé, J.; Cottancin, E.; Pellarin, M.; Treilleux, M.; Perez, A.; Vialle, J. L.; Broyer, M. Optical Properties of Gold Clusters in the Size Range 2−4 nm. *Phys. Rev. B* **1998**, *57*, 1963−1970.

(13) Prodan, E.; Nordlander, P.; Halas, N. J. Effects of Dielectric Screening on the Optical Properties of Metallic Nanoshells. *Chem. Phys. Lett.* **2003**, *368*, 94−101.

(14) Stener, M.; Nardelli, A.; De Francesco, R.; Fronzoni, G. Optical Excitations of Gold Nanoparticles: a Quantum Chemical Scalar Relativistic Time Dependent Density Functional Study. *J. Phys. Chem. C* **2007**, *111*, 11862−11871.

(15) Durante, N.; Fortunelli, A.; Broyer, M.; Stener, M. Optical Properties of Au Nanoclusters from TD-DFT Calculations. *J. Phys. Chem. C* **2011**, *115*, 6277−6282.

(16) Barcaro, G.; Broyer, M.; Durante, N.; Fortunelli, A.; Stener, M. Alloying Effects on the Optical Properties of Ag-Au Nanoclusters from TDDFT Calculations. *J. Phys. Chem. C* **2011**, *115*, 24085−24091.

(17) Guidez, E. B.; Mäkinen, V.; Häkkinen, H.; Aikens, C. M. Effects of Silver Doping on the Geometric and Electronic Structure and Optical Absorption Spectra of the Au $_{25-n}$Ag$_n$(SH)$_{18}^-$ (n = 1, 2, 4, 6, 8, 10, 12) Bimetallic Nanoclusters. *J. Phys. Chem. C* **2012**, *116*, 20617−20624.

(18) Walter, M.; Häkkinen, H.; Lehtovaara, L.; Puska, M.; Enkovaara, J.; Rostgaard, C.; Mortensen, J. J. Time-Dependent Density-Functional Theory in the Projector Augmented-Wave Method. *J. Chem. Phys.* **2008**, *128*, 244101 (1−10)..

(19) Koivisto, J.; Malola, S.; Kumara, C.; Dass, A.; Hakkinen, H.; Pettersson, M. Experimental and Theoretical Determination of the Optical Gap of the Au$_{144}$(SC$_2$H$_4$Ph)$_{60}$ Cluster and the (Au/Ag)$_{144}$(SC$_2$H$_4$Ph)$_{60}$ Nanoalloys. *J. Phys. Chem. Lett.* **2012**, *3*, 3076−3080.

(20) Yasuike, T.; Nobusada, K. Raman Enhancement by Plasmonic Excitation of Structurally-Characterized Metal Clusters: Au$_8$, Ag$_8$, and Cu$_8$. *Phys. Chem. Chem. Phys.* **2013**, *15*, 5424−5429.

(21) Marques, M. A. L.; Castro, A.; Bertsch, G. F.; Rubio, A. Octopus: a First-Principles Tool for Excited Electron−Ion Dynamics. *Comput. Phys. Commun.* **2003**, *151*, 60−78.

(22) Castro, A.; Marques, M. A. L.; Appel, H.; Oliveira, M.; Rozzi, C.; Andrade, X.; Lorenzen, F.; Gross, E. K. U.; Rubio, A. Octopus: a Tool for the Application of Time-Dependent Density Functional Theory. *Phys. Status Solidi B* **2006**, *243*, 2465−2488.

(23) Weissker, H.-Ch.; Mottet, C. Optical Properties of Pure and Core-Shell Noble-Metal Nanoclusters from TDDFT: The Influence of the Atomic Structure. *Phys. Rev. B* **2011**, *84*, 165443 (1−8)..

(24) Lozano, X. L.; Mottet, C.; Weissker, H.-Ch. Effect of Alloying on the Optical Properties of Ag−Au Nanoparticles. *J. Phys. Chem. C* **2013**, *117*, 3062−3068.

(25) Casida, M. E. *Recent Advances in Density-Functional Methods*; Chong, D. P., Ed.; World Scientific: Singapore, 1995; p 155.

(26) Johnson, H. E.; Aikens, C. M. Electronic Structure and TDDFT Optical Absorption Spectra of Silver Nanorods. *J. Phys. Chem. A* **2009**, *113*, 4445−4450.

(27) Liao, M.-S.; Bonifassi, P.; Leszczynski, J.; Ray, P. C.; Huang, M.-J.; Watts, J. D. Structure, Bonding, and Linear Optical Properties of a Series of Silver and Gold Nanorod Clusters: DFT/TDDFT Studies. *J. Phys. Chem. A* **2010**, *114*, 12701−12708.

(28) Guidez, E. B.; Aikens, C. M. Theoretical Analysis of the Optical Excitation Spectra of Silver and Gold Nanowires. *Nanoscale* **2012**, *4*, 4190−4198.

(29) Lian, K.; Sałek, P.; Jin, M.; Ding, D. Density-Functional Studies of Plasmons in Small Metal Clusters. *J. Chem. Phys.* **2009**, *130*, 174701 (1−6)..
(30) Bernadotte, S.; Evers, F.; Jacob, C. R. Plasmons in Molecules. *J. Phys. Chem. C* **2013**, *117*, 1863−1878.
(31) Pazos_Perez, N.; Baranov, D.; Irsen, S.; Hilgendorff, M.; Liz-Marzan, L.; Giersing, M. Article Synthesis of Flexible, Ultrathin Gold Nanowires in Organic Media. *Langmuir* **2008**, *24*, 9855−9860.
(32) Halder, A.; Ravishankar, N. Ultrafine Single-Crystalline Gold Nanowire Arrays by Oriented Attachment. *Adv. Mater.* **2007**, *19*, 1854−1858.
(33) Baerends, E. J.; Ellis, D. E.; Ros, P. Self-Consistent Molecular Hartree—Fock—Slater Calculations I. The Computational Procedure. *Chem. Phys.* **1973**, *2*, 41−51.
(34) Fonseca Guerra, C.; Snijders, J. G.; te Velde, G.; Baerends, E. J. Towards an Order-N DFT Method. *Theor. Chem. Acc.* **1998**, *99*, 391−403.
(35) Pyykkö, P. Theoretical Chemistry of Gold. *Angew. Chem., Int. Ed.* **2004**, *43*, 4412−4456.
(36) van Lenthe, E.; Baerends, E. J.; Snijders, J. G. Relativistic Regular Two-Component Hamiltonians. *J. Chem. Phys.* **1993**, *99*, 4597−4610.
(37) van Gisbergen, S. J. A.; Snijders, J. G.; Baerends, E. J. Implementation of Time-Dependent Density Functional Response Equations. *Comput. Phys. Commun.* **1999**, *118*, 119−138.
(38) Gross, E. K. U.; Kohn, W. Time-Dependent Density-Functional Theory. *Adv. Quantum Chem.* **1990**, *21*, 255−291.
(39) Van Leeuwen, R.; Baerends, E. J. Exchange-Correlation Potential with Correct Asymptotic Behavior. *Phys. Rev. A* **1994**, *49*, 2421−2431.
(40) van Gisbergen, S. J. A.; Kootstra, F.; Schipper, P. R. T.; Gritsenko, O. V.; Snijders, J. G.; Baerends, E. J. Density-Functional-Theory Response-Property Calculations with Accurate Exchange-Correlation Potentials. *Phys. Rev. A* **1998**, *57*, 2556−2571.
(41) Zangwill, A.; Soven, P. Density-Functional Approach to Local-Field Effects in Finite Systems: Photoabsorption in the Rare Gases. *Phys. Rev. A* **1980**, *21*, 1561−1572.
(42) Cottancin, E.; Celep, G.; Lermé, J.; Pellarin, M.; Huntzinger, J. R.; Vialle, J. L.; Broyer, M. Optical Properties of Noble Metal Clusters as a Function of the Size: Comparison Between Experiments and a Semi-Quantal Theory. *Theor. Chem. Acc.* **2006**, *116*, 514−523.